Convolution Neural Network for Brain Tumor Segmentation

Dr.G.Sivakumar[1] (Professor of CSE), R.Dharani[2], N.Kavenesh[3], S.Nandhakumar[4],
[1234]Dept of CSE, Erode Sengunthar Engineering College,
Erode, Tamil Nadu.

ABSTRACT

Magnetic Resonance Imaging (MRI) has grown in popularity in recent years, particularly in the field of medical technology, for the diagnosis of brain tumors. Only using MR imaging to detect and partition brain cancers requires a significant amount of time and effort on the side of the involved staff, as well as a high level of competence. This supports the requirement for developing an independent model for brain tumor diagnosis. In our work, we develop a convolutional neural network (CNN) for MR image-based brain tumor diagnosis. The dataset used in this study includes 253 brain MR pictures, of which 155 are said to include malignancies. Our approach has a 96% overall accuracy in identifying the MR pictures with malignancies. In the test dataset, the model performed better than the currently used traditional approaches for the diagnosis of brain tumors (Precision = 0.97, Recall = 0.96, and F1-score = 0.96). In order to speed up the treatment process, clinical specialists may find it useful to use the proposed model to determine whether the patient has a brain tumor.

Keyword - *Brain tumor, Segmentation, Medical imaging, Convolution neural network, MRI*

1. INTRODUCTION

An aberrant cell mass that forms a tumor as a result of unchecked cell division might impair the tissue or organ's ability to function normally [1]. Tumors can be identified based on their cell types and origin. Early tumor stages are primarily seen in the cerebrum portion of the brain, but secondary tumor stages (metastatic) travel from other parts of the body to the brain [2]. Malignant (high-grade), cancerous tumors can be benign or cancerous (low-grade). A high-grade brain tumor will expand very quickly and is more likely to infect nearby tissues than a benign brain tumor. Because of this, a primary high-grade brain tumor has a grim prognosis and significantly lowers quality of life and cognitive performance [3].

Brain and nervous system cancers are regarded to be the third most common malignancy among adults and teenagers, and they are tenth in the list of the most common causes of death [4]. Patients with a malignant brain have a 34% and 36% five-year survival rate, respectively. Nearly 80% of malignant cases in adults are gliomas, the most common kind of cerebral tumor [2, 3]. Low-grade glioma (LGG) patients have a ten-year survival rate that is generally around 57% [5]. Brain tumors can develop for a variety of reasons, including environmental factors like overuse of synthetic chemicals or genetics. Chemotherapy, surgery, and radiotherapy are available as treatments.

Early detection of a brain tumor not only increases the chances of survival but also provides more treatment options for patients. A brain tumor may be diagnosed using a variety of techniques, including an MRI scans, BIOPSY and SPECT scan. The most common technique is magnetic resonance imaging (MRI), a non-invasive imaging technology that offers distinct tissue contrast. In terms of normalizing tissue contrast, it is also very conformable and offers fine details of interest. The size, shape, and location of brain tumors are unpredictable, random, and irregular, which poses restrictions. Additionally, given the complexity and length of the task, non-autonomous splitting of the tumors is time-consuming, difficult, and mostly subjective.

The algorithms used to segment brain tumors can be divided into deep-learning techniques as well as conventional or non-autonomous methods. CAD systems using computing methods including K-means clustering, Principal Component Analysis, and Support Vector Machines, as well as regularised non-negative matrix factorization, are examples of the former [6], [7]. By combining fuzzy clustering and region-growing, Hsieh et al.

[8] were able to segment instances T1- and T2-weighted sequences are used to scan the body with an accuracy of 73%. Albarracin et al. demonstrated that Gaussian hidden Markov random field approach outperformed K-means, fuzzy k-means, and Gaussian mixture models by 77% accuracy. [9] in their evaluation of several clustering algorithms for brain tumor segmentation. [10] graded brain tumors using the SVM as a foundation, merging 38 first or second-order statistical measurements. Researchers are drawn to the deep learning (DL) based techniques that have recently been created since they are automated and draw their features directly from data [11].

Tumor segmentation was carried out in the study [12] utilising the LinkNet network. First, a single LinkNet network was used to segment all seven training datasets. Later, a technique for CNN was created to automatically extract the most common tumor types with no need for preprocessing. The results of the dice were 0.73 for a single network and 0.79 for several systems. The study [13] inputs the 3-D MRI image voxels into a 2-D CNN model in order to segment brain tumors using several convolutional neural networks. The result is a segmentation of brain tumors, not a categorization. Coupled SVMs with Artificial Neural Networks to grade brain cancers (ANNs) [14]. With a reduction in effective learning error, ANNs produced accuracy of 90.44%. The training portion of this approach uses a very limited number of images, which raises concerns about how well it would perform on datasets with many more images. Le et al. conducted studies on the ImageNet dataset [15]. By applying CNN theory, they created an object detector that achieved significantly better results than previous studies on the ImageNet dataset, improving the performance by nearly 70%.

In this case, a deep convolutional neural network (DCNN) built on a previously trained network is suggested. The VGG-16 classification model is pre-trained using the ImageNet dataset. Two kinds of brain MRI pictures make up the dataset that was used. The model produces better outcomes than traditional approaches. Section II of the article provides a more detailed discussion of the proposed methods. Section III provides an overview of the performance assessment, experimental findings, and the result comparison with traditional methods.

2. PROPOSED METHODOLOGY

The objective of the project is to automatically identify brain cancers in brain MRI pictures. Figure 2 shows the suggested approach's workflow in detail. Our proposed method for brain tumor detection from MRI images is based on CNN architecture and involves multiple steps. The input image is initially collected from the brain MRI. After applying picture thresholding and dilations to remove noise, data normalisation is carried out. The compiled database of brain MRI pictures is enhanced and processed. The photos were then scaled for the model's input and classified into two classes YES and NO—using a pretrained CNN and VGG-16. VGG-16 is one of the most advanced image classification networks, and a modified version of VGGNet trained on the ImageNet dataset is used here.

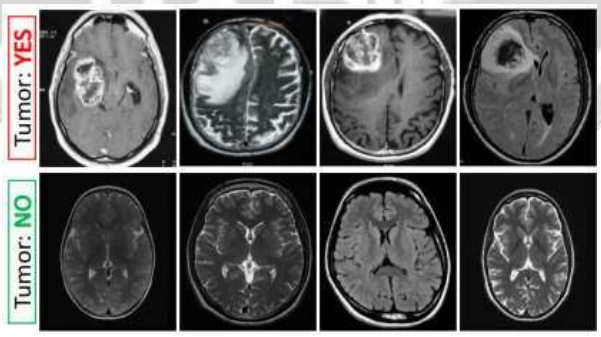

Fig. 1. Brain MRI images dataset sample

Brain MRI scan images make up the database used in this investigation. There are 253 different sized raw photos in total. The pictures were gathered from brain MRI image collections on Kaggle [16]. The file format is JPG. Based on the existence of tumors, the dataset is divided into the YES and NO classes. The remaining 98 photos are of normal brains, leaving 155 photographs with brain tumors overall. The dataset's example photos are shown in Figure 1.

2.1 Preprocessing and Dataset Splitting

Due to subject motions during acquisition or MRI machine restrictions, Anomalies in MR images can include non - uniformity distortions and motion heterogeneity. These artefacts introduce erroneous intensity rates, resulting in false - positive with in image. To deal with these artefacts, the N4ITK system's bias field distortion correction is applied. First, preprocessing was applied once the MRI picture was supplied. Because the black corners of the intensity values in MR images vary, it is difficult for CNN to get used to the specifics of each class designation. As a result, intensity levels are normalised to bring them closer to a steady state where the mean value goes to zero and the variance tends towards one in order to improve contrast. The photos are initially quantized using a given threshold of 45 to remove any little patches of noise. After that, a series of fissures and cervical dilation are used. The photos are then normalised by clipping the greatest contour of each one to the top, bottom, left, and right extraordinary points. Figure 3 shows the general normalisation procedure. The output i_0 comes from Eq. (1)

$$i_0 = \frac{i - \mu_i}{\sigma_i} \#(1)$$

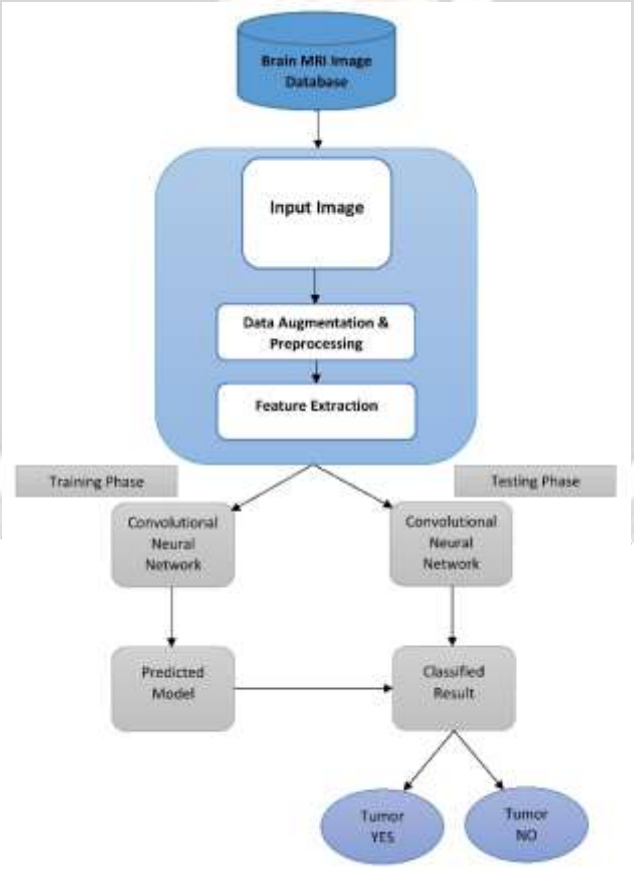

Fig. 2. The proposed method workflow

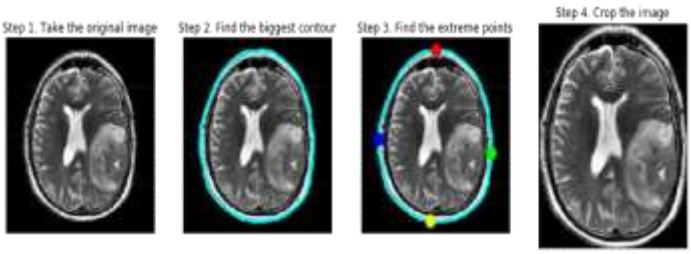

Fig. 3. Brain MRI images sample dataset

Here, *i* indicates a normalized version of input MRI image, μi is the mean and σ_i is the standard deviation.

The input layer of the VGG16 network has a size of 224x224. Data augmentation is used to reduce the size of our dataset and make it suitable for categorization. This is a common technique in deep learning that helps generate the required samples. By improving it, it also increases the network's effectiveness for a small database. Data augmentation helps the network function better by purposefully producing additional training data with the help of the initial data. To address the relatively small size of the dataset, the images are augmented to introduce greater variability. To reduce variance in the small dataset, we use image augmentation techniques with the Keras Image Data Generator during training. The photos are rotated randomly by 15 degrees during the entirety of the augmentation stage (clockwise). Additionally, they are displaced to 10% of their height and width values. Additionally, a range of 0 to 50% brightness or darkness is randomly applied to the photos. The images are likewise subjected to compressive with a 0.1 radian angle (counter-clockwise). The photos are then arbitrarily rotated both horizontally and vertically. Figure 4 displays the resized test photos used to train the model.

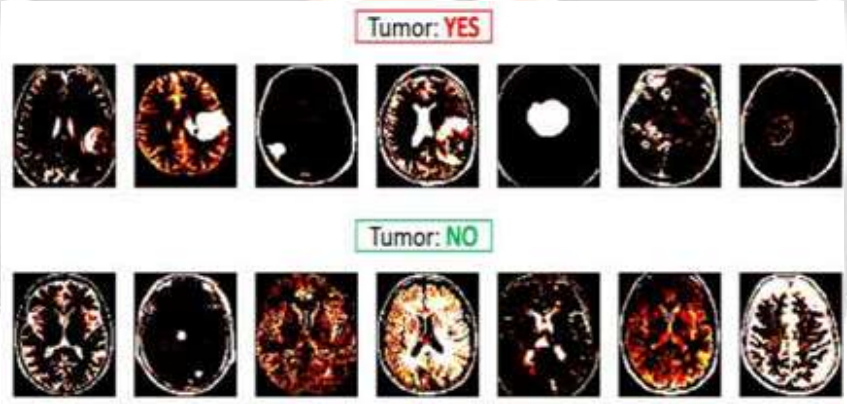

Fig. 4. Resized MRI images of the brain

An 80:10:10 ratio is used to partition the database into training, testing, and validation sets. The 253-image dataset is divided into 207, 24, and 22 image training, testing, and validation sets, respectively.

2.2 Convolutional Neural Networks (CNN): VGG16

An effective way to extract key features from images, analyse those features, and categorise them is to use convolutional neural networks (CNNs). Compared to traditional deep learning models, CNNs are better suited for image categorization tasks. Although there are numerous other CNN structures, the basic CNN architecture consists of three main layers: the convolution layer, the pooling layer, and the fully connected layer. Convolutional layers only function on a certain location and not everywhere. This process separates the features from the original data and transforms the previous layer into the next layer. The pooling layer then incorporates the knowledge from the previous layer to simplify the task. The fully linked layer executes the features that have been gathered from all preceding layers to produce the necessary categorised outputs.

In this investigation, features are extracted using the VGG-16. The VGG-16 model, based on CNN architecture and trained on large datasets such as ImageNet containing at least one million images, is highly acclaimed for its

effectiveness in image recognition. Simonyan and Zisserman of the Visual Geometry Group proposed the VGG-16 architecture during the ImageNet Competition in 2014, which is shown in the Figure 5. Their contributions earned them first and second place in the classification and mapping the categories, respectively.

The VGG-16 neural network was trained on a million annotated images and can classify images into 1000 categories. Its architecture comprises a total of 41 layers, out of which 16 have learnable parameters. The architecture includes 13 convolutional layers, three fully-connected layers, ReLU activation, and hidden layer capabilities. Convolution layers in the VGG-16 general model have 1 pixel padding and convolution stride and 3x3 filters (small receptive field) correspondingly. A max-pooling layer comes after every convolution layer.

The VGG-16 model takes input images of size 224x224, which are processed by the first two convolutional layers. The 64 feature kernel filters in the first two convolution layers have a size of 3x3 and a convolution stride or 1-pixel padding size. The new dimension of the resulting feature map is 224x224x64, which is transmitted to a max-pooling layer made up of kernels with a stride size of 2 and kernels with a size of 2x2 as well. The previous layer's feature map's spatial dimension, which was 112x112x128, is cut in half because when max-pooling layer has been applied over a 2x2 kernel space with a stride size of two pixels. The output is routed to the third and fourth convolution layers, which contain 124 functionality kernel filter layers with 3x3 dimensions, following movement through to the max-pooling layer. After passing through the third and fourth. After the convolutional layers, the output is fed into a max-pooling layer with a stride size of two pixels and a space of two kernels. This results in a feature map with dimensions of 56x56x256. The fifth, sixth, and seventh convolution layers, each of which includes 256 feature kernel filters of size 3x3, propagate the feature map.

After these layers, a second max-pooling is conducted over a layer with a stride size of two pixels and a space of two kernels to create a feature map with a dimension of 28 by 28 by 512. The following two sets of convolution layers, from the eighth to the thirteenth, have filters with a 3 by 3 grid size and 512 different feature maps. They are followed by max-pooling layers, which perform over a 2 by 2 kernel space with a stride size of one pixel.

The VGG-16 model's last layers consist of three fully connected (FC) layers with filter sizes of 3x3 and ReLU activation units of 4096, 4096, and 1000, respectively.

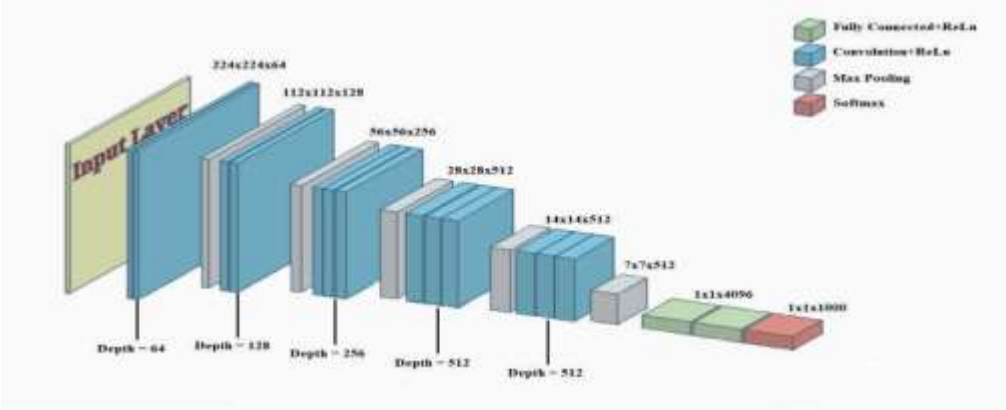

Fig. 5. Architecture of VGG16 Model

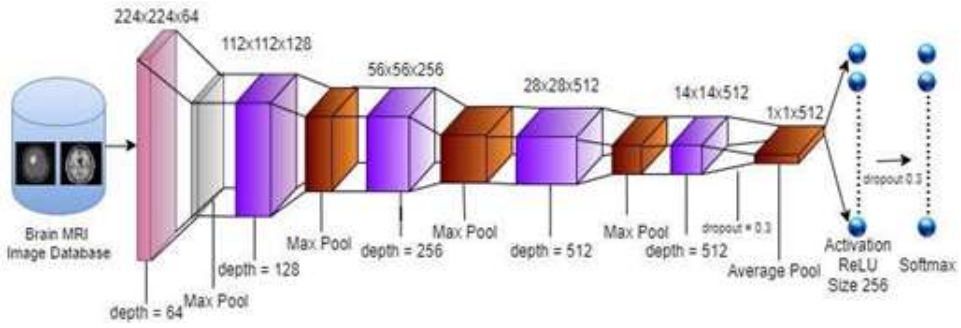

Fig. 6. The proposed CNN model Architecture

The ReLU can be expressed mathematically as follows,

$$f(x) = \max(0, x) \#(2)$$

The Softmax layer of 1000 units receives the feature vectors for classification from the Fully-Connected layers with their assistance. The Softmax activation function is described in equation three.

$$\sigma(z)_x = \frac{e^{z_x}}{\sum_i^l e^{z_i}} \#(3)$$

2.3 Proposed CNN Model Architecture

For this study, a pre-trained VGG-16 neural network model was used for classification, which had been trained on over one million annotated images from large datasets like ImageNet. The architecture has been altered for our research. The proposed model, as shown in Figure 6, is similar to the general VGG-16 model, but the structure has been modified to meet our challenge requirements. The last max-pooling layer from a standard VGG-16 design is swapped out for an avg pooling layer in the suggested model. By decreasing the total number of parameters in the model, the avg pooling layer, sometimes referred to as the Global Avg Pooling Layer (GAP), To avoid over - fitting, the feature map is spatially pooled. However, average-pooling reduces the spatial dimensions in a more significant way.

Replacing the max-pool layer with a GAP layer resulted in significantly improved results. Additionally, the middle set of convolution operations, immediately before the fully connected layers, to allow the backpropagation technique to work cannot be conducted while the layer weights are changed. Modifications may be made to the fully connected and GAP layers, though. The neural network's training time is greatly improved by freezing the early layers. Additionally, two dropout values of 0.3 have been added between the GAP layer and the fully connected layers to reduce overfitting and hence generalisation error. Finally, two Softmax layers with two channels each and completely connected layers each with 256 channels were employed.

3. RESULT ANALYSIS AND DISCUSSION

Eighty percent of the total data was set aside for training, ten percent for validation, and the remaining ten percent for testing in our fine-tuned CNN, VGG-16. The neural network is trained using the Adam optimizer with a learning rate of 0.0001 for 80 iterations, a batch size of 16, and the category cross-entropy loss function. In our testing, a computer system with a Geforce RTX 3080Ti used. The Intel 4th Xeon-2969, Core i7-3.4GHz CPU, 16 GB RAM, and Python in the Keras module were used to evaluate the CNN model.

3.1 Models Performance Evaluation

This section discusses the performance evaluation of the used and trained CNN model. The proposed model in this study was applied to the Brain MRI dataset, which contains 253 brain MR images, 155 of which show tumor indications. Instead of solely focusing on the classification accuracy as a model performance evaluating metric, is

used to clarify the superiority of the proposed approach as the dataset is distorted, along with precision, sensitivity, or recall, F1-score, average precision-recall score, Cohen's Kappa and other metrics.

The parameters TP and TN represent the true positive (TP) and true negative (TN) for the number of correctly diagnosed positive brain tumor images, respectively. In contrast, FP stands for false-positive images, which are the number of positive photos that were mistakenly categorized as negative, and FN stands for false-negative images, which are the number of negative images that were mistakenly classed as positive. Equation 4 can be used to determine the overall accuracy.

$$Accuracy(\%) = (TP + TN)/(TP + FP + TN + FN) \#(4)$$

However, as was already said, the F1-score values as well as the precision, sensitivity, or recall as well as the performance of the CNN model are also assessed. Formulae 5, 6, 7, and 12 each contain the equations for these metrics. The accuracy of the classifier model is represented by the precision value. The recall value, on the other hand, is a measure of how complete the model was.

$$Precision(PPV) = TP/(TP + FP) \#(5)$$

$$Sensitivity = TP/(TP + FN) \#(6)$$

$$F1 - Score = \frac{2 \times (Precision \times Recall)}{Precision + Recall} \#(7)$$

$$p_0 = \frac{TP + TN}{TP + FN + FP + TN} \#(8)$$

$$P_{yes} = \frac{TP + TN}{TP + FN + FP + TN} \cdot \frac{TP + FP}{TP + FN + FP + TN} \#(9)$$

$$P_{no} = \frac{FP + TN}{TP + FN + FP + TN} \cdot \frac{FN + TN}{TP + FN + FP + TN} \#(10)$$

$$P_e = P_{yes} + P_{no} \#(11)$$

$$Cohen's\ Kappa = \frac{P_0 - P_e}{1 - P_e} \#(12)$$

Table I gives the corresponding values for the measures used to evaluate performance. The suggested CNN method does a good job of locating the brain tumor in MR images. The model not only demonstrated a higher F1-score (97%) and greater precision-recall values (93%), which are indicators of the model's performance, but also higher classification accuracy (96%).

	precision	recall	f1-score	support
no	0.91	1.00	0.95	10
yes	1.00	0.94	0.97	16
accuracy			0.96	26
macro avg	0.95	0.97	0.96	26
weighted avg	0.97	0.96	0.96	26

```
[[10  0]
 [ 1 15]]
```

Fig. 7. Summary

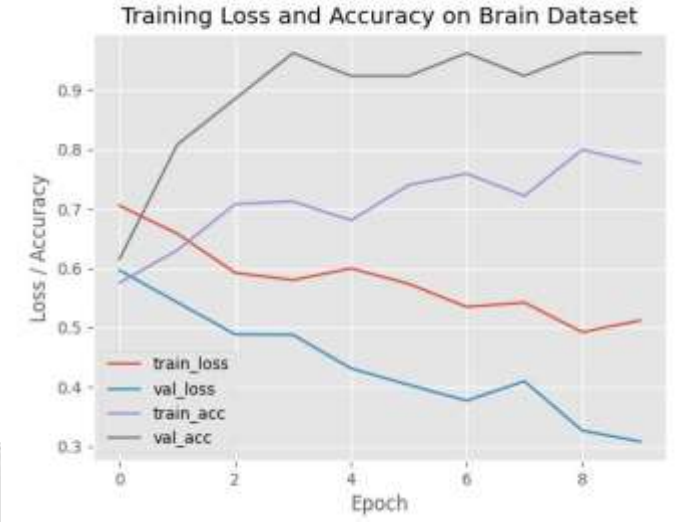

Fig. 8. Train loss and Accuracy graph

Table I. Performance of The Proposed CNN Model

Performance evaluating metrics	Performance score
Precision	0.97
Recall	0.94
F1-score	0.96
Cohen's Kappa	0.91
Accuracy	0.9615

3.2 Performance comparison with the existing method

The effectiveness of the model was evaluated by contrasting our suggested CNN classifier with established methods. The model's performance in comparison to other developed algorithms is shown in Table III. Our suggested model performs better than the earlier developed techniques, with accuracy of 96.15% shown in Figure.9 and Table.2.

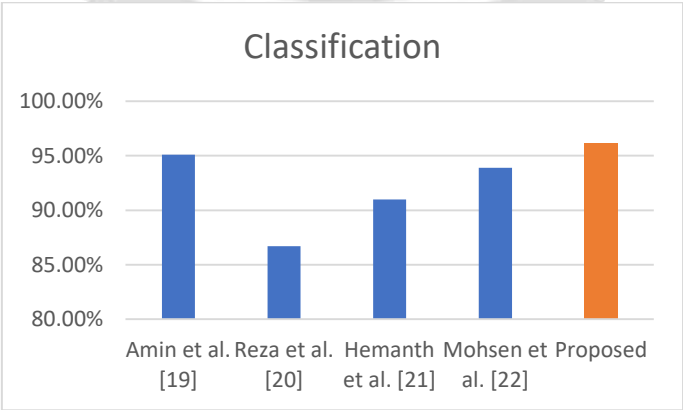

Fig. 9. Classification Accuracy

Table.2. Performance of the Proposed CNN Model

Method	Algorithms	Classification Accuracy
Amin et al. [19]	7 layered 2D CNN	95.1%
Reza et al. [20]	MFDFA + random Forest	86.7%
Hemanth et al. [21]	LinkNet	91.0%
Mohsen et al. [22]	SMO + SVM	93.9%
Proposed	**CNN (VGG16)**	**96.15%**

4. CONCLUSION

Medical therapies often benefit from the early detection of brain tumors. Due to the wide range of variances in medical images, it is essential to their processing. The automatic brain tumor detection approach makes diagnosis simple and greatly increases the likelihood that the patient will survive. The accuracy of tumor identification and classification has increased as a result of the application of CNN models is used for treating and diagnosing for brain cancers. The most common applications of MRI are for the diagnosis and grading of brain cancers. Using acquired brain MRI images, a deep neural convolution network (CNN) is created in this study to automatically identify the brain tumor. A pre-trained VGG-16 network was utilized to train the model quickly and efficiently on a limited amount of data. By using transfer learning and fine-tuning, the pre-trained network was able to recognize features in the brain MRI images relevant to tumor detection. This approach not only saves time but also improves the accuracy of the model. Results revealed that, in contrast to traditional methods, the network's proposed topology is alluring and performs especially well in tumor detection. To increase the effectiveness of the model, a number of preprocessing techniques were carried out. The model's overall classification accuracy of 96.15%, precision of 0.96, sensitivity of 0.94, and F1-score of 0.97, Cohen's Kappa 0.91 are supported by the results. As a result, the suggested framework might be put into use as a practical approach for physicians to offer desirable medical therapies for the early diagnosis of brain tumors. Our study is expected to be expanded in the future to include 3D brain images to determine the precise location of the tumor using CNN.

5. REFERENCES

[1] T. Logeswari and M. Karnan, "An improved implementation of brain tumor detection using segmentation based on hierarchical self-organizing map," *Int. J. Comput. Theory Eng.*, vol. 2, no. 4,p. 591, 2010.

[2] S. Bauer, R. Wiest, L.-P. Nolte, and M. Reyes, "A survey of MRI-based medical image analysis for brain tumor studies," *Phys. Med. Biol.*, vol. 58, no. 13, p. R97, 2013.

[3] J. A. Schwartzbaum, J. L. Fisher, K. D. Aldape, and M. Wrensch, "Epidemiology and molecular pathology of glioma," *Nat. Clin. Pract. Neurol.*, vol. 2, no. 9, pp. 494–503, 2006.

[4] J. Cheng *et al.*, "Retrieval of brain tumors by adaptive spatial pooling and fisher vector representation," *PLoS One*, vol. 11, no.6, p. e0157112, 2016.

[5] R. Ramakrishna, A. Hebb, J. Barber, R. Rostomily, and D. Silbergeld, "Outcomes in reoperated low-grade gliomas," *Neurosurgery*, vol. 77, no. 2, pp. 175–184, 2015.

[6] N. Sauwen *et al.*, "A semi-automated segmentation framework for MRI based brain tumor segmentation using regularized nonnegative matrix factorization," in *2016 12th International Conference on Signal-Image Technology & Internet-Based Systems (SITIS)*, 2016, pp. 88–95.

[7] M. K. Abd-Ellah, A. I. Awad, A. A. M. Khalaf, and H. F. A. Hamed, "Design and implementation of a computer-aided diagnosis system for brain tumor classification," in *2016 28th International Conference on Microelectronics* (ICM), 2016, pp. 73–76.

[8] T. M. Hsieh, Y.-M. Liu, C.-C. Liao, F. Xiao, I.-J. Chiang, and J.-M. Wong, "Automatic segmentation of meningioma from non- contrasted brain MRI integrating fuzzy clustering and region growing," *BMC Med. Inform. Decis. Mak.*, vol. 11, no. 1, p. 54, 2011.

[9] J. Juan-Albarrac\'\in *et al.*, "Automated glioblastoma segmentation based on a multiparametric structured unsupervised classification," *PLoS One*, vol. 10, no. 5, p. e0125143, 2015.

[10] M. Soltaninejad, X. Ye, G. Yang, N. Allinson, T. Lambrou, and others, "Brain tumour grading in different MRI protocols using SVM on statistical features," 2014.

[11] S. Pereira, A. Pinto, V. Alves, and C. A. Silva, "Brain tumor segmentation using convolutional neural networks in MRI images," *IEEE Trans. Med. Imaging*, vol. 35, no. 5, pp. 1240– 1251, 2016.

[12] Z. Sobhaninia *et al.*, "Brain tumor segmentation using deep learning by type specific sorting of images," *arXiv Prepr. arXiv1809.07786*, 2018.

[13] R. Lang, L. Zhao, and K. Jia, "Brain tumor image segmentation based on convolution neural network," in *2016 9th International Congress on Image and Signal Processing, BioMedical Engineering and Informatics (CISP-BMEI)*, 2016, pp. 1402– 1406.

[14] R. Ahmmed, A. Sen Swakshar, M. F. Hossain, and M. A. Rafiq, "Classification of tumors and it stages in brain MRI using support vector machine and artificial neural network," in *2017 International Conference on Electrical, Computer and Communication Engineering (ECCE)*, 2017, pp. 229–234.

[15] Q. V Le, "Building high-level features using large scale unsupervised learning," in *2013 IEEE international conference on acoustics, speech and signal processing*, 2013, pp. 8595– 8598.

[16] N. Chakrabarty, "Brain MRI Images for Brain Tumor Detection." Version, 2019.

[17] K. Simonyan and A. Zisserman, "Very deep convolutional networks for large-scale image recognition," *arXiv Prepr. arXiv1409.1556*, 2014.

[18] M. M. R. Khan, M. Siddique, A. Bakr, and S. Sakib, "Non- Intrusive Electrical Appliances Monitoring and Classification using K-Nearest Neighbors," *arXiv Prepr. arXiv1911.13257*, 2019.

[19] J. Amin, M. Sharif, M. Yasmin, and S. L. Fernandes, "Big data analysis for brain tumor detection: Deep convolutional neural networks," *Futur. Gener. Comput. Syst.*, vol. 87, pp. 290–297, 2018.

[20] S. M. S. Reza, R. Mays, and K. M. Iftekharuddin, "Multi-fractal detrended texture feature for brain tumor classification," in *Medical Imaging 2015: Computer-Aided Diagnosis*, 2015, vol. 9414, p. 941410.

[21] G. Hemanth, M. Janardhan, and L. Sujihelen, "Design and Implementing Brain Tumor Detection Using Machine Learning Approach," in *2019 3rd International Conference on Trends in Electronics and Informatics (ICOEI)*, 2019, pp. 1289–1294.

[22] H. Mohsen, E. A. El-Dahshan, E. M. El-Horbaty, and A. M. Salem, "Brain tumor type classification based on support vector machine in magnetic resonance images," *Ann. "Dunarea Jos" Univ. Galati, Math. Physics, Theor. Mech. Fascicle II, Year IX*, no. 1, 2017.